JOURNAL OF THEORETICAL AND APPLIED MECHANICS
53, 2, pp. 453-466, Warsaw 2015
DOI: 10.15632/jtam-pl.53.2.453

FREE VIBRATION AND BUCKLING ANALYSIS OF HIGHER ORDER LAMINATED COMPOSITE PLATES USING THE ISOGEOMETRIC APPROACH

Ognjen Peković, Slobodan Stupar, Aleksandar Simonović,
Jelena Svorcan, Srđan Trivković

University of Belgrade, Faculty of Mechanical Engineering, Serbia

e-mail: opekovic@mas.bg.ac.rs

This research paper presents a higher order isogeometric laminated composite plate finite element formulation. The isogeometric formulation is based on NURBS (non-uniform rational B-splines) basis functions of varying degree. Plate kinematics is based on the third order shear deformation theory (TSDT) of Reddy in order to avoid shear locking. Free vibration and the buckling response of laminated composite plates are obtained and efficiency of the method is considered. Numerical results with different element order are presented and the obtained results are compared to analytical and conventional numerical results as well as existing isogeometric plate finite elements.

Keywords: isogeometric, laminated composite plate, third order shear deformation theory

1. Introduction

Laminated composites are widely used in aerospace, marine and wind turbine industries. Recently, there has appeared a great number of general industrial products made of composites. The reasons for this are high strength-to-weight ratio, high stiffness, good dimensional stability after manufacturing and high impact, fatigue and corrosion resistance of composites. In addition to this, composite laminates possess ability to follow complex mould shapes and to be specifically tailored through optimization of ply numbers and fibre orientations through the structure so that they can meet specific needs while minimizing weight (Jones, 1999).

Laminates in general have thickness much smaller than their planar dimensions so one can use various plate theories instead of general 3D elasticity equations for their analysis (Reddy, 2004). Laminated plate theories are classified into three groups: 1) equivalent single layer theories (ESL), 2) layerwise plate theories and 3) individual-layer plate theories (Nosier *et al.*, 1993). The equivalent single layer theories are most widely used because they provide sufficiently accurate description of the global laminate response at low computational cost. Among ESL, the classical plate theory (CPT) is the simplest, but gives accurate results only for very thin plates since it is unable to capture transverse shear effects. The first order shear deformation theories (FSDT) give constant through thickness transverse shear strains resulting in constant transverse shear stresses through thickness, which is contradictory to the elasticity solution. In order to make up for this, one must use shear correction factors that are hard to determine. Higher order theories introduce additional unknown variables but are capable of modelling realistic transverse shear strains. Among them, the third order shear deformation theory of Reddy (1984) is the most popular among engineers. It uses quadratic variation of transverse shear strains with vanishing transverse shear stresses on the top and bottom surface, thus eliminating the need for the use of shear correction factors.

For arbitrary shapes and boundary conditions, the governing plate equations cannot be solved analytically. Among different numerical techniques that seek approximate solutions, the finite element method became a standard tool for treatment of stress analysis problems. In FEM, the unknown field variables are approximated by linear combination of interpolation (trial or shape) functions. In the standard FEM formulation, interpolation functions are locally defined polynomials inside the element and zero everywhere outside the considered element. Most existing finite elements and all commercial codes use Lagrangian (C^0 interelement continuity) and Hermitian (C^1 interelement continuity) basis functions.

A great need exists in industry for integration of the manufacturing process from conceptual phase and design (by means of computer-aided design (CAD)) through analysis (by using computer aided engineering (CAE) tools) to manufacturing (done on CNC machines trough computer aided manufacturing (CAM)). CAD and CAM industries rely on the use of NURBS geometry (Piegl, 1997; Rogers, 2001) for shape representation, thus CAD/CAM integration is relatively straightforward. Although specialized CAD/CAM/CAE systems exist for the last 20-25 years (PTC Creo, CATIA V5...) communication between CAD and CAE is not straightforward, and it is necessary to build a new finite element model in order to run the necessary analysis. This task takes up to 80% of total analysis time and is therefore one of the major bottlenecks in CAD/CAE/CAM integration (Cottrell *et al.*, 2009).

In order to overcome those difficulties, a new technique formally named isogeometric analysis is proposed (Hughes *et al.*, 2005). It allows the execution of analysis on geometrical CAD model. Instead of Lagrange or Hermit polynomial basis functions, the isogeometric finite element method relies on NURBS basis functions, same as almost every CAD or CAM package. NURBS offers general mathematical representation of both analytical geometric objects and freeform geometry. Recently, several research papers have appeared that used the isogeometric approach for plate and shell analysis (Kiendl *et al.*, 2009; Benson *et al.*, 2011; Echter *et al.*, 2013) and composite plate and shell analysis (Shojaee *et al.*, 2012; Thai *et al.*, 2012, 2013; Casanova and Gallego, 2013).

This paper presents free vibration and buckling analysis of TSDT composite plates in isogeometric framework. Isogeometric formulations of global stiffness, mass and geometrical stiffness matrix for quadratic, cubic and quartic elements are presented. All global matrices are formulated in full compliance with the TSDT of Reddy. Results are compared to other available data to demonstrate the accuracy of the proposed method.

2. NURBS curves, basis functions and surfaces

Non-uniform rational B-spline (NURBS) can represent arbitrary freeform shapes with analytical exactness that is needed in computer graphics (CG), CAD and CAM applications. After decades of technology improvement, NURBS provides users with great control over the object shape in an intuitive way with low memory consumption making them the most widespread technology for shape representation.

NURBS are generalizations of nonrational Bezier and nonrational B-splines curves and surfaces. Bezier curves are parametric polynomial curves defined as

$$C(u) = \sum_{i=0}^{n} B_{i,n}(u) P_i \qquad 0 \leqslant u \leqslant 1 \tag{2.1}$$

where $\{P_i\}$ are geometric coefficients (control points) and the $\{B_{i,n}(u)\}$ are the nth-degree Bernstein polynomials (basis or blending functions) defined as

$$B_{i,n}(u) = \frac{n!}{i!(n-i)!} u^i (1-u)^{n-i} \tag{2.2}$$

In order to accurately represent conic sections, it is necessary to use rational functions instead of polynomials, so the nth-degree rational Bezier curves are defined as follows

$$C(u) = \frac{\sum\limits_{i=0}^{n} B_{i,n}(u) w_i P_i}{\sum\limits_{i=0}^{n} B_{i,n}(u) w_i} \qquad 0 \leqslant u \leqslant 1 \tag{2.3}$$

where by $\{w_i\}$ we marked the weights that are scalar quantities.

The B-spline curve is a generalization of the Bezier curve defined as

$$C(u) = \sum_{i=0}^{n} N_{i,p}(u) P_i \qquad a \leqslant u \leqslant b \tag{2.4}$$

where $\{P_i\}$ are control points and $\{N_{i,p}(u)\}$ are the pth-degree B-spline basis functions (Fig. 1) that are defined on the nonuniform knot vector

$$\mathbf{U} = [\underbrace{a, \ldots, a}_{p+1}, u_{p+1}, \ldots, u_{m-p-1}, \underbrace{b, \ldots, b}_{p+1}] \tag{2.5}$$

The B-spline basis functions of the pth-degree are defined recursively

$$\begin{aligned} N_{i,0}(u) &= \begin{cases} 1 & u_i \leqslant u < u_{i+1} \\ 0 & \text{otherwise} \end{cases} \\ N_{i,p}(u) &= \frac{u - u_i}{u_{i+1} - u_i} N_{i,p-1}(u) + \frac{u_{i+p+1} - u}{u_{i+p+1} - u_{i+1}} N_{i+1,p-1}(u) \end{aligned} \tag{2.6}$$

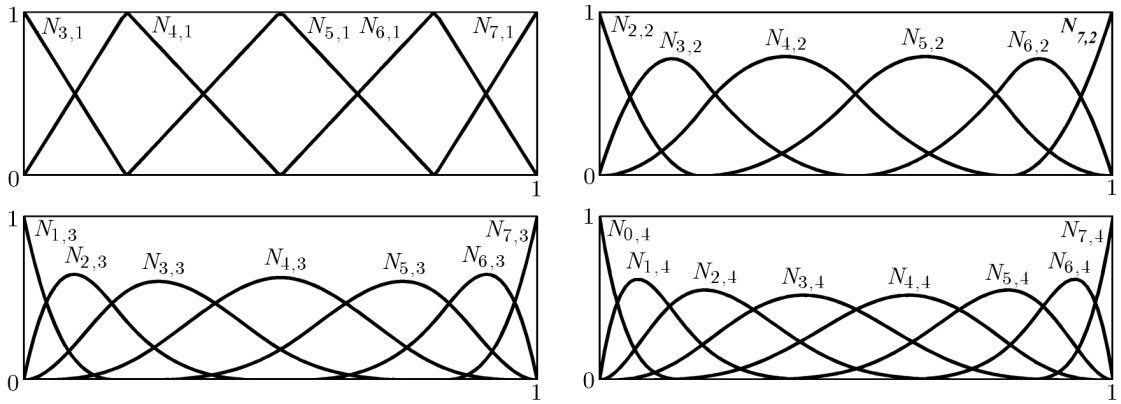

Fig. 1. Non-zero linear, quadratic, cubic and quartic B-spline basis functions defined on the open knot vector $\mathbf{U} = [\underbrace{0, \ldots, 0}_{p+1}, 0.2, 0.5, 0.8, \underbrace{1, \ldots, 1}_{p+1}]$

A rational representation of the B-spline curve is called a NURBS curve. A pth-degree NURBS curve is defined analogously to (2.3) as

$$C(u) = \frac{\sum\limits_{i=0}^{n} N_{i,p}(u) w_i P_i}{\sum\limits_{i=0}^{n} N_{i,p}(u) w_i} \qquad a \leqslant u \leqslant b \tag{2.7}$$

where $\{P_i\}$ are the control points, $\{w_i\}$ are the weights and $\{N_{i,p}(u)\}$ are the pth-degree B-spline basis functions that are defined on the nonuniform knot vector given by (2.5).

If we define the rational basis functions a

$$R_{i,p}(u) = \frac{N_{i,p}(u)w_i}{\sum\limits_{j=0}^{n} N_{j,p}(u)w_j} \tag{2.8}$$

we can write the NURBS curve as

$$C(u) = \sum_{i=0}^{n} R_{i,p}(u)P_i \tag{2.9}$$

It is easy to define multivariate NURBS basis functions by using the tensor product method. A NURBS surface of degree p in the u direction and degree q in the v direction is a bivariate vector-valued piecewise rational function of the form

$$S(u,v) = \sum_{i=0}^{n}\sum_{j=0}^{m} R_{i,j}^{p,q}(u,v)P_{i,j} = \frac{\sum\limits_{i=0}^{n}\sum\limits_{j=0}^{m} N_{i,p}(u)N_{j,q}(v)w_{i,j}P_{i,j}}{\sum\limits_{i=0}^{n}\sum\limits_{j=0}^{m} N_{i,p}(u)N_{j,q}(v)w_{i,j}} \qquad 0 \leqslant u,v < 1 \tag{2.10}$$

where $\{P_{i,j}\}$ are the control points, $\{w_{i,j}\}$ are the weights and $\{R_{i,j}^{p,q}(u,v)\}$ are the bivariate nonrational B-spline basis function defined on the nonuniform knot vectors

$$\mathbf{U} = [\underbrace{a,\ldots,a}_{p+1}, u_{p+1},\ldots,u_{r-p-1}, \underbrace{b,\ldots,b}_{p+1}] \qquad \mathbf{V} = [\underbrace{c,\ldots,c}_{q+1}, u_{q+1},\ldots,u_{s-q+1}, \underbrace{d,\ldots,d}_{q+1}] \tag{2.11}$$

where $r = n + p + 1$ and $s = m + q + 1$.

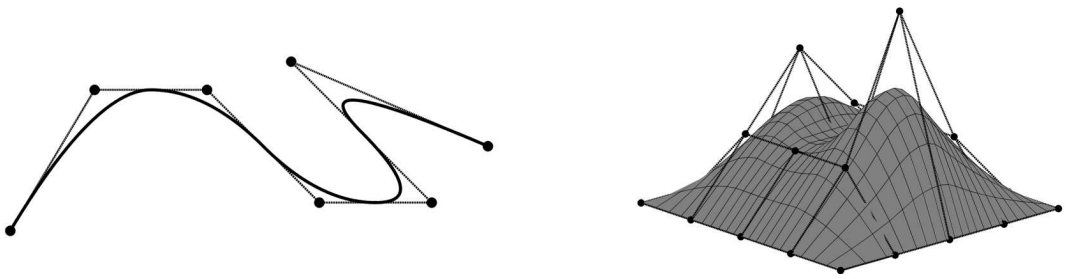

Fig. 2. Mesh of control points, the corresponding cubic NURBS curve (left) and NURBS surface (right)

3. Equations of motion

In the TSDT of Reddy (1984, 2004), the displacement field is defined as

$$\begin{aligned} u(x,y,z) &= u_0(x,y) + z\psi_x - \frac{4}{3h^2}z^3\Big(\psi_x + \frac{\partial w_0}{\partial x}\Big) \\ v(x,y,z) &= v_0(x,y) + z\psi_y - \frac{4}{3h^2}z^3\Big(\psi_y + \frac{\partial w_0}{\partial y}\Big) \\ w(x,y,z) &= w_0(x,y) \end{aligned} \tag{3.1}$$

where u_0, v_0, w_0 represent linear displacements of the midplane, ψ_x, ψ_y are rotations of normals to the midplane about the y and x-axes, respectively, and h denotes the total thickness of the laminate.

The in-plane strains $\{\varepsilon_{xx} \;\; \varepsilon_{yy} \;\; \gamma_{xy}\}^{\mathrm{T}}$ are given as

$$\boldsymbol{\varepsilon}_p = \begin{Bmatrix} \varepsilon_{xx} \\ \varepsilon_{yy} \\ \gamma_{xy} \end{Bmatrix} = \begin{Bmatrix} \varepsilon^0_{xx} \\ \varepsilon^0_{yy} \\ \gamma^0_{xy} \end{Bmatrix} + z \begin{Bmatrix} \varepsilon^1_{xx} \\ \varepsilon^1_{yy} \\ \gamma^1_{xy} \end{Bmatrix} + z^3 \begin{Bmatrix} \varepsilon^3_{xx} \\ \varepsilon^3_{yy} \\ \gamma^3_{xy} \end{Bmatrix} = \begin{Bmatrix} \dfrac{\partial u_0}{\partial x} \\ \dfrac{\partial v_0}{\partial y} \\ \dfrac{\partial u_0}{\partial y} + \dfrac{\partial v_0}{\partial x} \end{Bmatrix} + z \begin{Bmatrix} \dfrac{\partial \psi_x}{\partial x} \\ \dfrac{\partial \psi_y}{\partial y} \\ \dfrac{\partial \psi_x}{\partial y} + \dfrac{\partial \psi_y}{\partial x} \end{Bmatrix} - c_1 z^3 \begin{Bmatrix} \dfrac{\partial \psi_x}{\partial x} + \dfrac{\partial^2 w_0}{\partial x^2} \\ \dfrac{\partial \psi_y}{\partial y} + \dfrac{\partial^2 w_0}{\partial y^2} \\ \dfrac{\partial \psi_x}{\partial y} + \dfrac{\partial \psi_y}{\partial x} + 2\dfrac{\partial^2 w_0}{\partial x \partial y} \end{Bmatrix} \tag{3.2}$$

and the cross plane components $\{\gamma_{yz} \;\; \gamma_{xz}\}^{\mathrm{T}}$ as

$$\boldsymbol{\varepsilon}_s = \begin{Bmatrix} \gamma_{yz} \\ \gamma_{xz} \end{Bmatrix} = \begin{Bmatrix} \gamma^0_{yz} \\ \gamma^0_{xz} \end{Bmatrix} + z^2 \begin{Bmatrix} \gamma^0_{yz} \\ \gamma^0_{xz} \end{Bmatrix} = \begin{Bmatrix} \psi_y + \dfrac{\partial w_0}{\partial y} \\ \psi_x + \dfrac{\partial w_0}{\partial x} \end{Bmatrix} - c_2 z^2 \begin{Bmatrix} \psi_y + \dfrac{\partial w_0}{\partial y} \\ \psi_x + \dfrac{\partial w_0}{\partial x} \end{Bmatrix} \tag{3.3}$$

with $c_1 = 4/(3h^2)$ and $c_2 = 4/(h^2)$.

Constitutive relations between stresses and strains in the k-th lamina in the case of plane stress state, in the local coordinate system of the principle material coordinates (x_1, x_2, x_3), where x_1 is fibre direction, x_2 in-plane normal to fibre and x_3 normal to the lamina plane, are given by

$$\begin{Bmatrix} \sigma^{(k)}_1 \\ \sigma^{(k)}_2 \\ \tau^{(k)}_{12} \\ \tau^{(k)}_{23} \\ \tau^{(k)}_{13} \end{Bmatrix} = \begin{bmatrix} Q_{11} & Q_{12} & 0 & 0 & 0 \\ Q_{12} & Q_{22} & 0 & 0 & 0 \\ 0 & 0 & Q_{66} & 0 & 0 \\ 0 & 0 & 0 & Q_{44} & Q_{45} \\ 0 & 0 & 0 & Q_{45} & Q_{55} \end{bmatrix}^{(k)} \begin{Bmatrix} \varepsilon^{(k)}_1 \\ \varepsilon^{(k)}_2 \\ \gamma^{(k)}_{12} \\ \gamma^{(k)}_{23} \\ \gamma^{(k)}_{13} \end{Bmatrix} \tag{3.4}$$

The quantities $Q^{(k)}_{ij}$ are called the plane reduced stiffness components and are given in terms of material properties of each layer as

$$\begin{aligned} Q^{(k)}_{11} &= \frac{E^{(k)}_1}{1 - \nu^{(k)}_{12}\nu^{(k)}_{21}} & Q^{(k)}_{12} &= \frac{\nu^{(k)}_{12} E^{(k)}_2}{1 - \nu^{(k)}_{12}\nu^{(k)}_{21}} & Q^{(k)}_{22} &= \frac{E^{(k)}_2}{1 - \nu^{(k)}_{12}\nu^{(k)}_{21}} \\ Q^{(k)}_{66} &= G^{(k)}_{12} & Q^{(k)}_{44} &= G^{(k)}_{23} & Q^{(k)}_{55} &= G^{(k)}_{13} \end{aligned} \tag{3.5}$$

$E^{(k)}_1$, $E^{(k)}_2$ are Young's moduli, $\nu^{(k)}_{12}$, $\nu^{(k)}_{21}$ are Poisson's coefficients and $G^{(k)}_{12}$, $G^{(k)}_{23}$, $G^{(k)}_{13}$ are shear moduli of the lamina.

Composite laminates are usually made of several orthotropic layers (laminae) of different orientation. In order to express constitutive relations in the referent laminate (x, y, z) coordinate system (Fig. 3), the lamina constitutive relations are transformed as

$$\begin{Bmatrix} \sigma^{(k)}_{xx} \\ \sigma^{(k)}_{yy} \\ \tau^{(k)}_{xy} \\ \tau^{(k)}_{yz} \\ \tau^{(k)}_{xz} \end{Bmatrix} = \begin{bmatrix} \overline{Q}_{11} & \overline{Q}_{12} & \overline{Q}_{16} & 0 & 0 \\ \overline{Q}_{12} & \overline{Q}_{22} & \overline{Q}_{26} & 0 & 0 \\ \overline{Q}_{16} & \overline{Q}_{26} & \overline{Q}_{66} & 0 & 0 \\ 0 & 0 & 0 & \overline{Q}_{44} & \overline{Q}_{45} \\ 0 & 0 & 0 & \overline{Q}_{45} & \overline{Q}_{55} \end{bmatrix}^{(k)} \begin{Bmatrix} \varepsilon^{(k)}_{xx} \\ \varepsilon^{(k)}_{yy} \\ \gamma^{(k)}_{xy} \\ \gamma^{(k)}_{yz} \\ \gamma^{(k)}_{xz} \end{Bmatrix} \tag{3.6}$$

where $\overline{Q}_{ij}$ are the lamina plane stress reduced stiffness components in the laminate coordinate system defined as (Reddy, 2004)

$$\begin{Bmatrix} \overline{Q}_{11} \\ \overline{Q}_{22} \\ \overline{Q}_{16} \\ \overline{Q}_{26} \\ \overline{Q}_{66} \end{Bmatrix}^{(k)} = \begin{bmatrix} m^4 & n^4 & 2m^2n^2 & 4m^2n^2 \\ n^4 & m^4 & 2m^2n^2Q_{12} & 4m^2n^2 \\ m^3 & -mn^3 & mn^3 - m^3n & 2(mn^3 - m^3n) \\ mn^3 & -m^3n & m^3n - mn^3 & 2(m^3n - mn^3) \\ m^2n^2 & m^2n^2 & -2m^2n^2 & (m^2 - n^2)^2 \end{bmatrix}^{(k)} \begin{Bmatrix} Q_{11} \\ Q_{22} \\ Q_{12} \\ Q_{66} \end{Bmatrix}^{(k)}$$
$$\begin{Bmatrix} \overline{Q}_{44} \\ \overline{Q}_{45} \\ \overline{Q}_{55} \end{Bmatrix}^{(k)} = \begin{bmatrix} m^2 & n^2 \\ -mn & mn \\ n^2 & m^2 \end{bmatrix}^{(k)} \begin{Bmatrix} Q_{44} \\ Q_{55} \end{Bmatrix}^{(k)} \tag{3.7}$$

with m and n denote cosine and sine of the angle θ between the global axis x and local axis x_1 (Fig. 3).

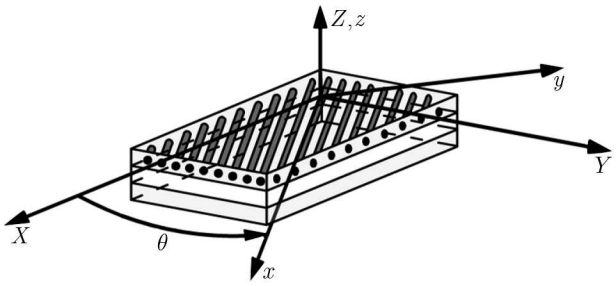

Fig. 3. Local and global coordinate systems of a laminate

The dynamic form of the principle of virtual work in matrix form is given by

$$\int_{\Omega} \delta\boldsymbol{\varepsilon}_p^{\mathrm{T}} \boldsymbol{\mathcal{D}} \boldsymbol{\varepsilon}_p \, d\Omega + \int_{\Omega} \delta\boldsymbol{\varepsilon}_s^{\mathrm{T}} \boldsymbol{\mathcal{D}}^s \boldsymbol{\varepsilon}_s \, d\Omega = \int_{\Omega} \delta\mathbf{u}^{\mathrm{T}} \mathbf{m}\, \ddot{\mathbf{u}} \, d\Omega \tag{3.8}$$

where $\mathbf{m}$ is defined as

$$\mathbf{m} = \begin{bmatrix} I_0 & 0 & 0 & J_1 & 0 & -c_1 I_3 & 0 \\ 0 & I_0 & 0 & 0 & J_1 & 0 & -c_1 I_3 \\ 0 & 0 & I_0 & 0 & 0 & 0 & 0 \\ J_1 & 0 & 0 & K_2 & 0 & -c_1 I_4 & 0 \\ 0 & J_1 & 0 & 0 & K_2 & 0 & -c_1 I_4 \\ -c_1 I_3 & 0 & 0 & -c_1 I_4 & 0 & c_1^2 I_6 & 0 \\ 0 & -c_1 I_3 & 0 & 0 & -c_1 I_4 & 0 & c_1^2 I_6 \end{bmatrix} \tag{3.9}$$

with

$$(I_0, I_1, I_2, I_3, I_4, I_6) = \sum_{k=1}^{N} \int_{-h/2}^{h/2} \rho^{(k)} (1, z, z^2, z^3, z^4, z^6) \, dz$$
$$J_1 = I_1 - c_1 I_3 \qquad K_2 = I_2 - 2c_1 I_4 + c_1^2 I_6$$

Matrices that relate the stress resultants to the strains are given as

$$\boldsymbol{\mathcal{D}} = \begin{bmatrix} \mathbf{A} & \mathbf{B} & \mathbf{E} \\ \mathbf{B} & \mathbf{D} & \mathbf{F} \\ \mathbf{E} & \mathbf{F} & \mathbf{H} \end{bmatrix} \qquad \boldsymbol{\mathcal{D}}^s = \begin{bmatrix} \mathbf{A}^s & \mathbf{D}^s \\ \mathbf{D}^s & \mathbf{F}^s \end{bmatrix} \tag{3.10}$$

with

$$
\begin{aligned}
(A_{ij}, B_{ij}, D_{ij}, E_{ij}, F_{ij}, H_{ij}) &= \sum_{k=1}^{N} \int_{-h/2}^{h/2} \overline{Q}_{ij}^{(k)} (1, z, z^2, z^3, z^4, z^6)\, dz \\
(A_{ij}^s, D_{ij}^s, F_{ij}^s) &= \sum_{k=1}^{N} \int_{-h/2}^{h/2} \overline{Q}_{ij}^{(k)} (1, z^2, z^4)\, dz \\
\mathbf{u}^{\mathrm{T}} &= \left\{ u_0 \quad v_0 \quad w_0 \quad \psi_x \quad \psi_y \quad \frac{\partial w_0}{\partial x} \quad \frac{\partial w_0}{\partial y} \right\}^{\mathrm{T}}
\end{aligned}
\tag{3.11}
$$

For buckling analysis, the weak form of the virtual work principle in the matrix form is stated as

$$
\begin{aligned}
&\int_{\Omega} \delta\boldsymbol{\varepsilon}_p^{\mathrm{T}} \boldsymbol{\mathcal{D}} \boldsymbol{\varepsilon}_p \, d\Omega + \int_{\Omega} \delta\boldsymbol{\varepsilon}_s^{\mathrm{T}} \boldsymbol{\mathcal{D}}^s \boldsymbol{\varepsilon}_s \, d\Omega + h \int_{\Omega} \begin{bmatrix} \nabla^{\mathrm{T}} \delta u_0 & \nabla^{\mathrm{T}} \delta v_0 & \nabla^{\mathrm{T}} \delta w_0 \end{bmatrix} \begin{bmatrix} \widehat{\boldsymbol{\sigma}}_0 & 0 & 0 \\ 0 & \widehat{\boldsymbol{\sigma}}_0 & 0 \\ 0 & 0 & \widehat{\boldsymbol{\sigma}}_0 \end{bmatrix} \begin{bmatrix} \nabla u_0 \\ \nabla v_0 \\ \nabla w_0 \end{bmatrix} d\Omega \\
&\quad + \frac{h^3}{12} \int_{\Omega} \begin{bmatrix} \nabla^{\mathrm{T}} \delta\psi_x & \nabla^{\mathrm{T}} \delta\psi_y \end{bmatrix} \begin{bmatrix} \widehat{\boldsymbol{\sigma}}_0 & 0 \\ 0 & \widehat{\boldsymbol{\sigma}}_0 \end{bmatrix} \begin{bmatrix} \nabla\psi_x \\ \nabla\psi_y \end{bmatrix} d\Omega = 0
\end{aligned}
\tag{3.12}
$$

where $\nabla^{\mathrm{T}} = \begin{bmatrix} \partial/\partial x & \partial/\partial y \end{bmatrix}$ is the gradient operator and $\widehat{\boldsymbol{\sigma}}_0 = \begin{bmatrix} \sigma_x^0 & \tau_{xy}^0 \\ \tau_{xy}^0 & \sigma_y^0 \end{bmatrix}$ is the matrix of in-plane pre-buckling stresses.

4. Isogeometric finite element formulation of TSDT laminated plate

In TSDT, the field variables are inplane displacements, transverse displacements and rotations at control points. By using isogeometric paradigm, the same NURBS basis functions that are used to describe plate geometry are used for the interpolation of field variables

$$
\mathbf{u} = \begin{Bmatrix} u_0 \\ v_0 \\ w_0 \\ \psi_x \\ \psi_y \end{Bmatrix} = \sum_{I=1}^{n\times m} \begin{bmatrix} N_I & 0 & 0 & 0 & 0 \\ 0 & N_I & 0 & 0 & 0 \\ 0 & 0 & N_I & 0 & 0 \\ 0 & 0 & 0 & N_I & 0 \\ 0 & 0 & 0 & 0 & N_I \end{bmatrix} \begin{Bmatrix} u_{0I} \\ v_{0I} \\ w_{0I} \\ \psi_{xI} \\ \psi_{yI} \end{Bmatrix} = \sum_{I=1}^{n\times m} N_I q_I
\tag{4.1}
$$

where $n \times m$ is the number of control points (basis functions), N_I are rational basis functions and q_I are degrees of freedom associated with the control point I.

The in-plane strains and shear strains are obtained using Eqs. (3.2),(3.3) and (4.1) as

$$
\boldsymbol{\varepsilon}_p = \sum_I [\mathbf{B}_I^0 + z\mathbf{B}_I^1 - c_1 z^3 \mathbf{B}_I^3] \mathbf{q}_I \qquad \boldsymbol{\varepsilon}_s = \sum_I [\mathbf{B}_I^{S0} - c_2 z^2 \mathbf{B}_I^{S2}] \mathbf{q}_I
\tag{4.2}
$$

where

$$
\begin{aligned}
\mathbf{B}^0 &= \begin{bmatrix} N,x & 0 & 0 & 0 & 0 \\ 0 & N,y & 0 & 0 & 0 \\ N,y & N,x & 0 & 0 & 0 \end{bmatrix} \qquad \mathbf{B}^1 = \begin{bmatrix} 0 & 0 & 0 & N,x & 0 \\ 0 & 0 & 0 & 0 & N,y \\ 0 & 0 & 0 & N,y & N,x \end{bmatrix} \\
\mathbf{B}^3 &= \begin{bmatrix} 0 & 0 & N,xx & N,x & 0 \\ 0 & 0 & N,yy & 0 & N,y \\ 0 & 0 & 2N,xy & N,y & N,x \end{bmatrix}
\end{aligned}
\tag{4.3}
$$

and

$$\mathbf{B}^{S0} = \mathbf{B}^{S2} = \begin{bmatrix} 0 & 0 & N,y & 0 & N \\ 0 & 0 & N,x & N & 0 \end{bmatrix} \tag{4.4}$$

where N,x and N,y denote the first and N,xx, N,yy, N,xy second derivatives of N with respect to x and y.

For free vibration analysis, we can write

$$(\mathbf{K} - \omega^2 \mathbf{M})\mathbf{q} = \mathbf{0} \tag{4.5}$$

and for buckling analysis, we get

$$(\mathbf{K} - \lambda_{cr}\mathbf{K}_g)\mathbf{q} = \mathbf{0} \tag{4.6}$$

where $\mathbf{K}$ is the global stiffness matrix defined as

$$\mathbf{K} = \int_{\Omega} \begin{bmatrix} \mathbf{B}^0 \\ \mathbf{B}^1 \\ \mathbf{B}^3 \end{bmatrix}^{\mathrm{T}} \begin{bmatrix} \mathbf{A} & \mathbf{B} & \mathbf{E} \\ \mathbf{B} & \mathbf{D} & \mathbf{F} \\ \mathbf{E} & \mathbf{F} & \mathbf{H} \end{bmatrix} \begin{bmatrix} \mathbf{B}^0 \\ \mathbf{B}^1 \\ \mathbf{B}^3 \end{bmatrix} + \begin{bmatrix} \mathbf{B}^{s0} \\ \mathbf{B}^{s2} \end{bmatrix}^{\mathrm{T}} \begin{bmatrix} \mathbf{A}^s & \mathbf{D}^s \\ \mathbf{D}^s & \mathbf{F}^s \end{bmatrix} \begin{bmatrix} \mathbf{B}^{s0} \\ \mathbf{B}^{s2} \end{bmatrix} \, d\Omega \tag{4.7}$$

The global mass matrix $\mathbf{M}$ is given by

$$\mathbf{M} = \int_{\Omega} \mathbf{N}_m^{\mathrm{T}} \mathbf{m}\, \mathbf{N}_m \, d\Omega \tag{4.8}$$

with

$$\mathbf{N}_m = \begin{bmatrix} N_I & 0 & 0 & 0 & 0 & 0 & 0 \\ 0 & N_I & 0 & 0 & 0 & 0 & 0 \\ 0 & 0 & N_I & 0 & 0 & N_I,x & N_I,y \\ 0 & 0 & 0 & N_I & 0 & 0 & 0 \\ 0 & 0 & 0 & 0 & N_I & 0 & 0 \end{bmatrix}^{\mathrm{T}} \tag{4.9}$$

The global geometrical stiffness matrix $\mathbf{K}_g$ that takes into account the contribution of shear strains is given by

$$\mathbf{K}_g = \int_{\Omega} \mathbf{N}_g^{\mathrm{T}} \mathbf{I}_g \mathbf{N}_g \, d\Omega \tag{4.10}$$

with

$$\mathbf{N}_g = \begin{bmatrix} \nabla N & 0 & 0 & 0 & 0 \\ 0 & \nabla N & 0 & 0 & 0 \\ 0 & 0 & \nabla N & 0 & 0 \\ 0 & 0 & 0 & \nabla N & 0 \\ 0 & 0 & 0 & 0 & \nabla N \\ 0 & 0 & N_I,xx & N_I,x & 0 \\ 0 & 0 & N_I,xy & N_I,y & 0 \\ 0 & 0 & N_I,xy & 0 & N_I,x \\ 0 & 0 & N_I,yy & 0 & N_I,y \end{bmatrix} \qquad \mathbf{I}_g = \begin{bmatrix} \mathbf{I}_{g0} & 0 & 0 & 0 & 0 & 0 & 0 \\ 0 & \mathbf{I}_{g0} & 0 & 0 & 0 & 0 & 0 \\ 0 & 0 & \mathbf{I}_{g0} & 0 & 0 & 0 & 0 \\ 0 & 0 & 0 & \mathbf{I}_{g2} & 0 & \mathbf{I}_{g4} & 0 \\ 0 & 0 & 0 & 0 & \mathbf{I}_{g2} & 0 & \mathbf{I}_{g4} \\ 0 & 0 & 0 & \mathbf{I}_{g4} & 0 & \mathbf{I}_{g6} & 0 \\ 0 & 0 & 0 & 0 & \mathbf{I}_{g4} & 0 & \mathbf{I}_{g6} \end{bmatrix} \tag{4.11}$$

and

$$\nabla N = \begin{bmatrix} N_I,x & N_I,y \end{bmatrix}^{\mathrm{T}} \qquad \mathbf{I}_{g0} = h\widehat{\boldsymbol{\sigma}}_0 \qquad \mathbf{I}_{g2} = \frac{h^3}{12}\widehat{\boldsymbol{\sigma}}_0$$

$$\mathbf{I}_{g4} = \frac{h^5}{80}\begin{bmatrix} \sigma_x^0 & -\tau_{xy}^0 \\ -\tau_{xy}^0 & \sigma_y^0 \end{bmatrix} \qquad \mathbf{I}_{g6} = \frac{h^7}{448}\begin{bmatrix} \sigma_x^0 & -\tau_{xy}^0 \\ -\tau_{xy}^0 & \sigma_y^0 \end{bmatrix}$$

5. Free vibration analysis of laminated composite plates

In this Section, the performance of quadratic, cubic and quartic TSDT isogeometric elements in the free vibration analysis is studied. Standard benchmark problems with various plate shapes, boundary conditions, material characteristics and thickness are solved using the proposed method, and the results are compared to other available ones.

5.1. Square composite plates

We consider [0/90], [0/90/0] and [0/90/0/90] cross-ply laminates. Each ply is made of an orthotropic material with the following characteristics: $E_1 = 1.73 \cdot 10^5$ MPa, $E_2 = 3.31 \cdot 10^4$ MPa, $G_{12} = 9.38 \cdot 10^3$ MPa, $G_{13} = 8.27 \cdot 10^3$ MPa, $G_{23} = 3.24 \cdot 10^3$ MPa and $\nu_{12} = 0.036$. Mass density ρ is equal to one. The plate is simply supported on all edges, and all layers are assumed to be of the same thickness and density. The plates length-to-width ratio is $a/b = 1$ and the width-to-thickness ratio is $b/h = 10$. The normalized frequency is defined as $\overline{\omega} = (\omega h)\sqrt{\rho/E_2}$.

In Tables 1, 2 and 3, we present four dimensionless natural frequencies that correspond to the values of Fourier integers $m, n = 1, 2$ for [0/90], [0/90/0] and [0/90/0/90] laminates, respectively. We compare the results of quadratic, cubic and quartic IGA TSDT elements with the exact 3D elasticity solution and the analytical solutions of TSDT, FSDT and CPT theories given by Nosier *et al.* (1993). The shear correction factor for FSDT theory is taken to be $\pi^2/12$. In this example, the plate is modeled with 8x8 elements.

The results obtained with quadratic elements are in very good agreement with the analytical solution based on TSDT theory of Reddy. We see that the results obtained with cubic and quartic elements are quite similar and differ slightly from the quadratic elements solutions.

Table 1. Non-dimensional frequency parameter $\overline{\omega}$ of the [0/90] laminate

	Exact	TSDT	FSDT	CPT	IGA TSDT quadratic	IGA TSDT cubic	IGA TSDT quartic
$m, n = 1$	0.06027	0.06057	0.6038	0.06513	0.06056	0.06053	0.06053
$m, n = 1, 2$ $m, n = 2, 1$	0.14539	0.14681	0.14545	0.17744	0.14703	0.14664	0.14663
$m, n = 2$	0.20229	0.20482	0.20271	0.25814	0.20508	0.20449	0.20448

Table 2. Non-dimensional frequency parameter $\overline{\omega}$ of the [0/90/0] laminate

	Exact	TSDT	FSDT	CPT	IGA TSDT quadratic	IGA TSDT cubic	IGA TSDT quartic
$m, n = 1$	0.06715	0.06839	0.06931	0.07769	0.06837	0.06835	0.06835
$m, n = 1, 2$	0.12811	0.13010	0.12886	0.15185	0.13014	0.12993	0.12993
$m, n = 2, 1$	0.17217	0.17921	0.18674	0.26599	0.17957	0.17908	0.17907
$m, n = 2$	0.20798	0.21526	0.22055	0.31077	0.21551	0.21494	0.21494

5.2. Circular composite plates

Next, we consider a symmetric four-layer laminated circular plate with $[\theta^\circ/-\theta^\circ/-\theta^\circ/\theta^\circ]$ stacking sequence and clamped boundaries.

The material of each ply has the following characteristics: $E_1 = 40E_2$, $G_{12} = G_{13} = 0.6E_2$, $G_{23} = 0.5E_2$, $\nu_{12} = 0.25$, $\rho = 1$. Fiber orientation angles are $\theta = 0^\circ, 15^\circ, 30^\circ, 45^\circ$ and the

Table 3. Non-dimensional frequency parameter $\overline{\omega}$ of the [0/90/0/90] laminate

	Exact	TSDT	FSDT	CPT	IGA TSDT quadratic	IGA TSDT cubic	IGA TSDT quartic
$m, n = 1$	0.06621	0.06789	0.06791	0.07474	0.06787	0.06785	0.06785
$m, n = 1, 2$ $m, n = 2, 1$	0.15194	0.16065	0.16066	0.20737	0.16085	0.16048	0.16048
$m, n = 2$	0.20841	0.22108	0.22097	0.29824	0.22133	0.22077	0.22076

diameter-to-thickness ratio is 10. In order to represent the circular plate geometry, we used quadratic basis functions with knot vectors $\mathbf{U} = [0, 0, 0, 1, 1, 1]$ and $\mathbf{V} = [0, 0, 0, 1, 1, 1]$. We chose an appropriate control polygon in order to get a desirable distribution of the parametric curves. The control polygon and resulting mesh are shown in Fig. 4. The results for a 8×8 element mesh are presented in Table 4 and compared with the results obtained with MISQ20 elements (Nguyen-Van *et al.*, 2008), MLSDQ elements (Liew *et al.*, 2003) and the IGA FSDT results obtained by Thai *et al.* (2012). There is a good agreement between the results. The first six mode shapes of the quartic $[45°/-45°/-45°/45°]$ clamped laminated circular plate are shown in Fig. 5.

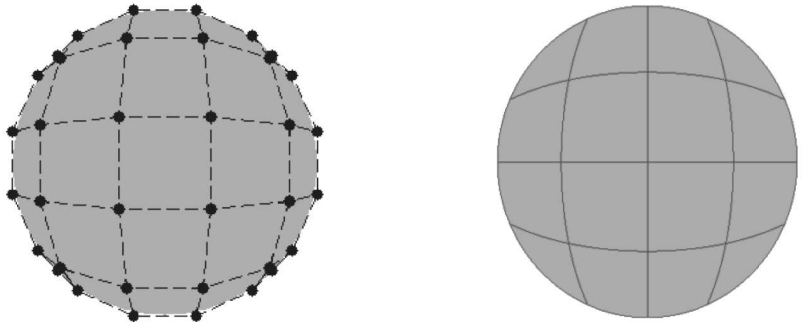

Fig. 4. The control polygon and knot plot of a quadratic circular plate with 4 non-zero knot spans

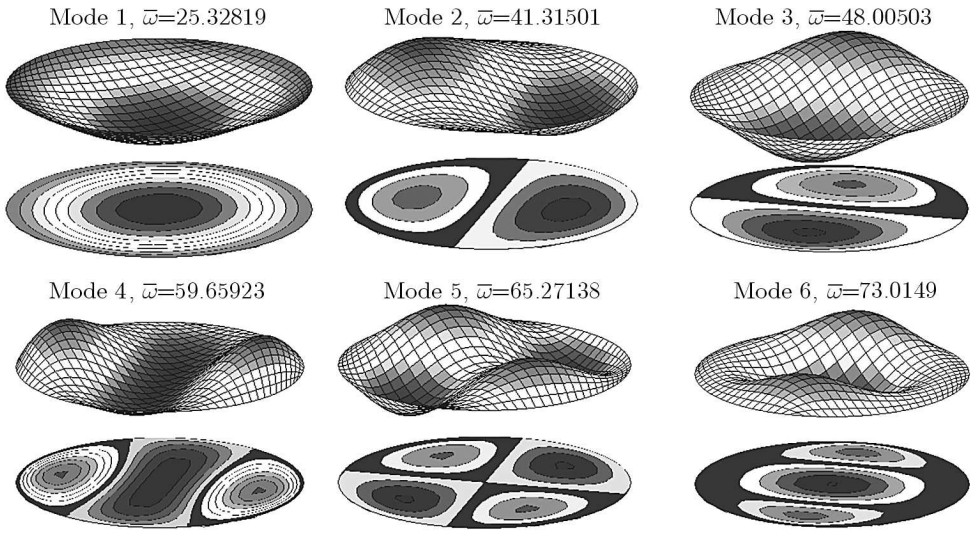

Fig. 5. First six mode shapes of a quartic $[45°/-45°/-45°/45°]$ clamped laminated circular plate

Table 4. Non-dimensional frequency parameter $\overline{\omega}$ of the $[\theta^\circ/-\theta^\circ/-\theta^\circ/\theta^\circ]$ circular laminated plate

θ°	Method	Modes					
		1	2	3	4	5	6
0°	FSDT – MISQ20	22.123	29.768	41.726	42.805	50.756	56.950
	FSDT – MLSDQ	22.211	29.651	41.101	42.635	50.309	54.553
	IGA FSDT quadratic	22.0989	29.5409	40.8126	42.5447	50.2975	54.7732
	IGA FSDT cubic	22.1110	29.5550	40.8150	42.5650	50.3201	54.7332
	IGA FSDT quartic	22.1227	29.5735	40.8410	42.5854	50.3478	54.7609
	IGA TSDT quadratic	22.8351	31.4480	45.5659	48.1996	49.5516	56.7189
	IGA TSDT cubic	22.6745	31.2413	45.3267	48.1985	49.4442	56.5244
	IGA TSDT quartic	22.6127	31.0741	45.0771	48.1983	49.4310	56.4541
15°	FSDT – MISQ20	22.698	31.568	43.635	44.318	53.468	60.012
	FSDT – MLSDQ	22.774	31.455	43.350	43.469	52.872	57.386
	IGA FSDT quadratic	22.6500	31.3012	43.3124	43.3833	52.8952	57.8347
	IGA FSDT cubic	22.6626	31.3166	43.3335	43.3899	52.9197	57.8064
	IGA FSDT quartic	22.6751	31.3359	43.3550	43.4165	52.9486	57.8349
	IGA TSDT quadratic	23.4537	33.6251	48.4304	49.4626	58.8442	66.4838
	IGA TSDT cubic	23.2857	33.4227	48.1945	49.3160	58.5463	66.1343
	IGA TSDT quartic	23.2140	33.2644	47.9875	49.3001	58.4857	65.9376
30°	FSDT – MISQ20	24.046	36.399	44.189	52.028	57.478	67.099
	FSDT – MLSDQ	24.071	36.153	43.968	51.074	56.315	66.220
	IGA FSDT quadratic	23.9428	35.9896	43.7948	50.9574	56.6770	66.0745
	IGA FSDT cubic	23.9565	36.0085	43.8164	50.9745	56.7038	66.1011
	IGA FSDT quartic	23.9703	36.0298	43.8390	51.0024	56.7337	66.1316
	IGA TSDT quadratic	24.9036	38.7086	48.9210	56.0703	62.7850	75.2087
	IGA TSDT cubic	24.7076	38.5058	48.7678	55.8127	62.4374	74.7126
	IGA TSDT quartic	24.6221	38.4000	48.7367	55.7171	62.3863	74.6206
45°	FSDT – MISQ20	24.766	39.441	43.817	57.907	57.945	66.297
	FSDT – MLSDQ	24.752	39.181	43.607	56.759	56.967	65.571
	IGA FSDT quadratic	24.6335	38.9379	43.4120	56.8708	56.9251	65.2751
	IGA FSDT cubic	24.6478	38.9591	43.4330	56.8937	56.9531	65.3002
	IGA FSDT quartic	24.6622	38.9814	43.4559	56.9205	56.9844	65.3320
	IGA TSDT quadratic	25.6205	41.4886	48.2065	59.9176	65.6484	73.5627
	IGA TSDT cubic	25.4140	41.3547	48.0552	59.6995	65.2816	73.0792
	IGA TSDT quartic	25.3282	41.3150	48.0050	59.6592	65.2714	73.0149

6. Buckling analysis of composite plate

6.1. Square plate under uniaxial compression

We consider a symmetric four-layer $[0^\circ/90^\circ/0^\circ/90^\circ]$ cross-ply plate with simply supported (SS-1) boundary conditions on all sides (Fig. 6). The plate material is the same as in the previous example. In Table 5, we present the convergence study of a dimensionless buckling load factor defined as $\overline{\lambda} = \lambda_{cr} a^2/(E_2 h^3)$ with the edge-to-thickness ratio equal to 10, where a is edge length, h is total thickness of the laminate, λ_{cr} is the critical load factor and E_2 is the elastic modulus. In Table 6, the results for different edge-to-thickness ratios and an 8×8 element mesh are compared with the analytical solutions based on CPT, FSDT and TSDT theories given by Reddy (2004) and with IGA FSDT solutions by Thai *et al.* (2012). The obtained results agree remarkably with the other available ones.

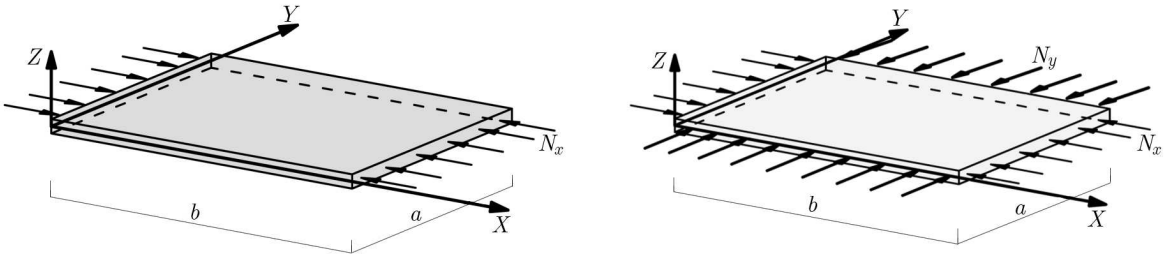

Fig. 6. Simply supported laminated plate under uniaxial (left) and biaxial (right) compression

Table 5. Normalized critical buckling load of the simply supported cross-ply [0°/90°/90°/0°]

Method	Mesh			
	4×4	8×8	16×16	32×32
IGA TSDT quadratic	23.2336	23.1725	23.1596	23.1563
IGA TSDT cubic	23.1563	23.1551	23.1551	23.1551
IGA TSDT quartic	23.1551	23.1551	23.1551	23.1551

Table 6. Normalized critical buckling load of the simply supported cross-ply [0°/90°/90°/0°] plate

Method	a/h				
	5	10	20	50	100
CPT (Khdeir and Librescu, 1988)	36.160	36.160	36.160	36.160	36.160
FSDT (Khdeir and Librescu, 1988)	11.575	23.453	31.707	35.356	35.955
TSDT (Khdeir and Librescu, 1988)	11.997	23.340	31.660	35.347	35.953
IGA FSDT quadratic (Thai *et al.*, 2012)	–	23.6599	31.8288	35.3945	36.0130
IGA FSDT cubic (Thai *et al.*, 2012)	–	23.6594	31.8267	35.3813	35.9617
IGA FSDT quartic (Thai *et al.*, 2012)	–	23.6594	31.8267	35.3813	35.9616
IGA TSDT quadratic	11.8270	23.1558	31.5738	35.3480	35.9807
IGA TSDT cubic	11.8135	23.1386	31.5541	35.3245	35.9474
IGA TSDT quartic	11.8134	23.1385	31.5540	35.3243	35.9468

6.2. Square plate under biaxial compression

The last numerical example in this paper considers a symmetric [0°/90°/0°] three-layer simply supported plate with the same material characteristics as in the previous example, subjected to the biaxial buckling load (Fig. 6). the dimensionless buckling factor is defined in the same way as in the uniaxial compression example. The results presented in Table 7 show the dimensionless buckling factor for different length-to-thickness ratios. The results obtained by the proposed method are in good agreement with CPT, FSDT and TSDT solutions by Khdeir and Librescu (1988).

7. Conclusions

The current investigation presents the isogeometric free vibration and buckling analysis of a laminated plate based on the TSDT theory of Reddy. TSDT is chosen in order to avoid the usage of shear correction factors. By using NURBS basis functions, the C1 continuity needed for the implementation of TSDT in FEM is easily achieved. It is relatively easy and straightforward to change the order of NURBS basis functions, so quadratic, cubic, quartic or higher order TSDT elements are easily formulated. The presented results are very accurate and close to analytical

Table 7. Normalized critical buckling load of the simply supported [0°/90°/0°] cross-ply plate under biaxial compression

Method	a/h				
	5	10	20	50	100
CPT (Khdeir and Librescu, 1988)	14.704	14.704	14.704	14.704	14.704
FSDT (Khdeir and Librescu, 1988)	1.427	5.492	10.202	12.192	13.146
TSDT (Khdeir and Librescu, 1988)	1.465	5.526	10.259	12.226	13.285
IGA TSDT quadratic	1.4262	5.2755	9.7590	11.9065	12.9697
IGA TSDT cubic	1.4198	5.2670	9.7455	11.8873	12.9437
IGA TSDT quartic	1.4198	5.2670	9.7453	11.8868	12.9428

TSDT solutions. It can be seen that for the free vibration and buckling analyses, cubic and quartic elements give very similar results, while quadratic elements provide slightly less accurate results. In our opinion, one can use cubic TSDT elements in order to obtain satisfactory results in the least computationally expensive way.

Isogeometric analysis is not confined only to NURBS basis functions. Since NURBS basis functions have several disadvantages from the point of view of analysis, such as the inability of local refinement, a considerable effort is invested in the research of T-splines (Bazilevs *et al.*, 2010), locally refined (LR) B-splines (Johannessen *et al.*, 2014), PHT splines (Nguyen-Thanh *et al.*, 2011), hierarchical refinement of NURBS (Schillinger *et al.*, 2012) and other technologies that are capable of local refinement in the context of isogeometric analysis.

In this paper, the proposed method is used on simple geometries, but it is possible to deal with more complex geometries by using T-spline technique or the bending strip method proposed by Kindl *et al.* (2010).

Acknowledgment

This work has been supported by the Ministry of Science and Technological Development of Republic of Serbia through Technological Development Project No. 35035.

References

1. Bazilevs Y., Calo V.M.,Cottrell J.A., Evans J.A., Hughes T.J.R., Lipton S., Scott M.A., Sederberg T.W., Isogeometric analysis using T-splines, *Computer Methods in Applied Mechanics and Engineering*, **199**, 229-263
2. Benson D.J., Bazilevs Y., Hsu M.C., Hughes T.J.R., 2011, Isogeometric shell analysis: the Reissner-Mindlin shell, *Computer Methods in Applied Mechanics and Engineering*, **199**, 5/8, 276-289
3. Casanova C., Gallego A., 2013, NURBS-based analysis of higher-order composite shells, *Composite Structures*, **104**, 125-133
4. Cottrell J.A., Hughes T.J.R., Bazilevs Y., 2009, *Isogeometric Analysis: Toward Integration of CAD and FEA*, John Wiley & Sons, Chichester
5. Echter R., Oesterle B., Bischoff M., 2013, A hierarchic family of isogeometric shell finite elements, *Computer Methods in Applied Mechanics and Engineering*, **254**, 170-180
6. Hughes T.J.R., Cottrell J.A., Bazilevs Y., 2005, Isogeometric analysis: CAD, finite elements, NURBS, exact geometry and mesh refinement, *Computer Methods in Applied Mechanics and Engineering*, **194**, 39/41, 4135-4195
7. Johannessen K.A., Kvamsdal T., Dokken T., 2014, Isogeometric analysis using LR B-splines, *Computer Methods in Applied Mechanics and Engineering*, **269**, 471-514

8. Jones R.M., 1999, *Mechanics of Composite Materials*, 2nd ed., Taylor & Francis, Philadelphia

9. Khdeir A.A, Librescu L., 1988, Analysis of symmetric cross-ply laminated elastic plates using a higher-order theory: Part II - Buckling and free vibration, *Composite Structures*, **9**, 4, 259-277

10. Kiendl J., Bazilevs Y., Hsu M.-C., Wchner R., Bletzinger K.-U., 2010, The bending strip method for isogeometric analysis of Kirchhoff–Love shell structures comprised of multiple patches, *Computer Methods in Applied Mechanics and Engineering*, **199**, 37/40, 2403-2416

11. Kiendl J., Bletzinger K.-U., Linhard J., Wchner R., 2009, Isogeometric shell analysis with Kirchhoff–Love elements, *Computer Methods in Applied Mechanics and Engineering*, **198**, 49/52, 3902-3914

12. Liew K.M., Huang Y.Q., Reddy J.N., 2003, Vibration analysis of symmetrically laminated plates based on FSDT using the moving least squares differential quadrature method, *Computer Methods in Applied Mechanics and Engineering*, **192**, 2203-2222

13. Nguyen-Thanh N., Kiendl J., Nguyen-Xuan H., Wchner R., Bletzinger K.U., Bazilevs Y., Rabczuk T., 2011, Rotation free isogeometric thin shell analysis using PHT-splines, *Computer Methods in Applied Mechanics and Engineering*, **200**, 47/48, 3410-3424

14. Nguyen-Van H., Mai-Duy N., Tran-Cong T., 2008, Free vibration analysis of laminated plate/shell structures based on FSDT with a stabilized nodal-integrated quadrilateral element, *Journal of Sound and Vibration*, **313**, 1/2, 205-223

15. Nosier A., Kapania R.K., Reddy J.N., 1993, Free vibration analysis of laminated plates using a layerwise theory, *AIAA Journal*, **31**, 12, 2335-2346

16. Piegl L., Tiller W., 1997, *The NURBS Book*, Springer-Verlag New York, New York

17. Reddy J.N., 1984, A simple higher-order theory for laminated composite plates, *Journal of Applied Mechanics*, **51**, 4, 745-752

18. Reddy J.N., 2004, *Mechanics of Laminated Composite Plates and Shells Theory and Anlysis*, 2nd ed., CRC Press, Boca Raton

19. Rogers D., 2001, *An Introduction to NURBS With Historical Perspective*, Morgan Kaufmann Publishers, San Francisco

20. Schillinger D., Dedè L., Scott M.A., Evans J.A., Borden M.J., Rank E., Hughes T.J.R., 2012, An isogeometric design-through-analysis methodology based on adaptive hierarchical refinement of NURBS, immersed boundary methods, and T-spline CAD surfaces, *Computer Methods in Applied Mechanics and Engineering*, **249/252**, 116-150

21. Shojaee S., Valizadeh N., Izadpanah E., Bui T., Vu T.-V., 2012, Free vibration and buckling analysis of laminated composite plates using the NURBS-based isogeometric finite element method, *Composite Structures*, **94**, 5, 1677-1693

22. Thai C., Ferreira A.J.M., Carrera E., Nguyen-Xuan H., 2013, Isogeometric analysis of laminated composite and sandwich plates using a layerwise deformation theory, *Composite Structures*, **104**, 196-214

23. Thai C.H., Nguyen-Xuan H., Nguyen-Xuan N., Le T-H., Nguyen-Thoi T., Rabczuk T., 2012, Static, free vibration, and buckling analysis of laminates composite Reissner-Mindlin plates using NURBS-based isogeometric approach, *International Journal for Numerical Methods in Engineering*, **91**, 6, 571-603

Manuscript received February 21, 2014; accepted for print November 30, 2014